




Article

Macrolides from *Streptomyces* sp. SN5452 and Their Antifungal Activity against *Pyricularia oryzae*

Yinan Wang¹, Di Yang¹, Yuhui Bi¹  and Zhiguo Yu^{1,2,*}¹ College of Plant Protection, Shenyang Agricultural University, Shenyang 110866, China² Engineering & Technological Research Center of Biopesticide for Liaoning Province, Shenyang 110866, China

* Correspondence: zyu@syau.edu.cn; Tel.: +86-24-88487148

Abstract: *Pyricularia oryzae* causes rice blast, the major destructive disease in nearly all rice fields. In order to obtain highly active compounds against *P. oryzae*, four new 20-membered macrolides named venturicidins G–J (1–4) were isolated from the culture broth of *Streptomyces* sp. SN5452 along with two known ones, venturicidins A (5) and B (6). Their structures were determined by the cumulative analyses of nuclear magnetic resonance (NMR) spectroscopy and high-resolution electrospray ionization mass spectrometry (HRESIMS) data. All isolated compounds were evaluated for their antifungal activity against *P. oryzae*. Interestingly, these compounds exhibited obvious inhibition to mycelial growth and conidial germination of *P. oryzae*. Remarkably, the EC₅₀ values of venturicidins A (5), B (6), and I (3) against mycelial growth were 0.11, 0.15 and 0.35 µg/mL, and their EC₅₀ values of conidial germination were 0.27, 0.39 and 1.14 µg/mL, respectively. The analysis of structure-activity relationships (SARs) revealed that the methylated positions might be involved in the antifungal activity of venturicidins. These results indicate that the venturicidins are prospective candidates for novel fungicides that can be applied in controlling rice blast.

Keywords: *Streptomyces*; macrolides; venturicidins; *Pyricularia oryzae*; antifungal activity

Citation: Wang, Y.; Yang, D.; Bi, Y.; Yu, Z. Macrolides from *Streptomyces* sp. SN5452 and Their Antifungal Activity against *Pyricularia oryzae*. *Microorganisms* **2022**, *10*, 1612. <https://doi.org/10.3390/microorganisms10081612>

Academic Editor: Mohamed Hijri

Received: 26 July 2022

Accepted: 8 August 2022

Published: 9 August 2022

Publisher's Note: MDPI stays neutral with regard to jurisdictional claims in published maps and institutional affiliations.



Copyright: © 2022 by the authors. Licensee MDPI, Basel, Switzerland. This article is an open access article distributed under the terms and conditions of the Creative Commons Attribution (CC BY) license (<https://creativecommons.org/licenses/by/4.0/>).

1. Introduction

The need for food quality and quantity is urgent due to the increase in population and the improvement of people's living standards [1]. Rice is the staple food for most peoples in different countries around the world [2], including China, Bangladesh, and Malaysia. However, the yield of rice is threatened by a variety of plant diseases every year, among which rice blast can cause up to 30% yield loss in some regions [3,4]. Rice blast is caused by *Pyricularia oryzae* [5], a haploid filamentous ascomycete [6,7], which can infect any stage of plant growth, causing leaf blast, node blast and panicle blast [8–11].

At present, the control of rice blast mainly depends on applying synthetic chemical agents [12,13]. These have been repeatedly applied for decades, which not only develops resistance of *P. oryzae* to them [14,15], but also destroys the balance of ecosystem [16]. Moreover, after several years of planting disease-resistant varieties [17], the pathogens may develop new pathogenic races, resulting in the collapse of resistance [11,18]. In order to solve these difficulties, scientists expect to seek for environmentally friendly and safe microbial biocontrol agents.

Actinomycetes, renowned for their ability to produce various novel bioactive compounds, were applied in the agricultural field as microbial biocontrol agents [19–21]. *Streptomyces* is the largest genus of the phylum *Actinobacteria*, which produces abundant secondary metabolites such as macrolides, terpenoids, alkaloids, flavones, and polyketides [22,23]. In previous studies, these secondary metabolites were considered as crop protection agents, due to their antimicrobial, insecticidal and herbicidal activities [24–27].

In our ongoing efforts to seek for new and bioactive secondary metabolites produced by actinomycetes [28,29], the crude extract from the fermentation culture of *Streptomyces* sp.

SN5452 at 50 µg/mL could completely inhibit the mycelial growth of *P. oryzae* (Figure S1). In this study, we isolated and purified the active compounds from the crude extract. The structures of these active compounds were determined based on the analysis of mass spectrometry (MS) and nuclear magnetic resonance (NMR) data. Furthermore, their antifungal activity against *P. oryzae* was also evaluated with mycelial growth inhibition and conidial germination assays.

2. Materials and Methods

2.1. General Experimental Procedures

Optical rotations were obtained at the sodium D line with a polarimeter (Atago, Tokyo, Japan), maintained at room temperature. NMR spectra experiments were operated on an Avance-600 NMR spectrometer (Bruker, Karlsruhe, Germany). Chemical shifts were calibrated by carbon signals and the residual proton signals of DMSO- d_6 (δ_C 39.5 and δ_H 2.50). High-resolution mass spectra (HRESIMS) were recorded on an Agilent 1260/6520 Q-TOF mass spectrometer. The crude extract was chromatographed on silica column with silica gel of 100–200 and 200–300 mesh (Qingdao Ocean Chemical Co., Ltd., Qingdao, China) and Sephadex LH-20 (GE Healthcare, Uppsala, Sweden). High-performance liquid chromatography (HPLC) analysis was performed using the C18 column (Agilent ZORBAX Eclipse XDB, 4.60 × 250 mm, 5 µm) on an Agilent 1260 series system (Agilent, Santa Clara, CA, USA). Active compounds were collected using semi-preparative HPLC with a C18 column (Agilent ZORBAX Eclipse XDB, 9.4 × 250 mm, 5 µm). The germination number of conidia was observed by microscope (Nikon, Tokyo, Japan). All chemical agents were purchased from Sinopharm Chemical Reagent company (Shanghai, China).

2.2. Actinomycete Material

The stain was isolated from the gut of millipede (*Kronopolites svenhedind* Verhoeff) which was obtained from campus of Shenyang Agricultural University. The processing of the Diplopoda gut sample and the isolation of the strain were conducted according to Heo et al.'s method [30]. For taxonomic identification, the strain 16S rRNA sequence was compared and analyzed by EzTaxon database. A phylogenetic tree was constructed based on 16S rRNA sequence using Molecular Evolutionary Genetics (MEGA v 7.0) [31,32]. Colonies were deposited in 20% (*v/v*) glycerol solution at −80 °C.

2.3. Fermentation and Extraction

Streptomyces sp. SN5452 was cultured on Gause's synthetic agar no. 1 (GS) [33] plates at 28 °C in the dark for 10 days for subsequent fermentation. The mycelia were inoculated into test tubes with 5 mL liquid ISP 2 medium [34] and shaken (180 rpm) at 28 °C in the dark for 2 days, and then were transferred to 250 mL Erlenmeyer flask with 50 mL liquid ISP 2 medium with shaking for 2 days to prepare the seed culture. Finally, the seed culture was shifted into 2 L Erlenmeyer flasks, which contained 400 mL of the GS liquid medium and 16 g of Amberlite XAD-16 resin. A total of 48 L fermentation culture was obtained after cultivating for 7 days under identical conditions.

The resin was collected from the fermentation broth by repeated deionized water washing. After it was dried in an oven at 30 °C to remove moisture, the resin was extracted four times with CH₃OH. The CH₃OH fractions were pooled and concentrated to obtain the CH₃OH extract, and then it was redissolved in 50% CH₃OH in H₂O (0.6 L). The solution was extracted four times with the same volume of CH₂Cl₂. Collecting CH₂Cl₂ fractions were concentrated to produce 11 g of crude extract.

2.4. Isolation and Purification

The purification of concentrated crude extract was operated by normal phase silica gel chromatography (6 cm × 40 cm), using a gradient of CH₃OH-CH₂Cl₂ solvent (100:0, 50:1, 25:1, 25:2, 25:4, 1:1 and 0:100, 2 L each) as the mobile phase, which produced three fractions, A–C. Fraction B was further fractionated via silica gel chromatography with

petroleum ether-ethyl acetate (7:3, 6.5:3.5, 6:4, 5.5:4.5 and 1:1, 1 L each) as the mobile phase to obtain B₁ and B₂ fractions. Fraction B₁ was purified using Sephadex LH-20 column with petroleum ether-dichloromethane-methanol (2:1:1) as eluent to remove impurities. Then, it was isolated by reverse-phase semipreparative HPLC, and eluted with 80% CH₃OH in H₂O to yield compounds **1** (3.2 mg, *t_R* = 18.04 min), **6** (71.5 mg, *t_R* = 19.86 min), and **2** (8.1 mg, *t_R* = 31.62 min). Fraction B₂ was also separated applying reverse-phase semipreparative HPLC with the same chromatographic separation conditions as fraction B₁, yielding compounds **5** (101.6 mg), **3** (4.5 mg) and **4** (10.3 mg) at 17.57, 20.57 and 26.36 min, respectively.

Venturicidin G, **1**. White powder; $[\alpha]_D^{24} + 33.33$ (c 0.3, CH₃OH); HRESIMS *m/z* 715.4400 [M + Na]⁺ (calcd for C₃₉H₆₄O₁₀Na, 715.4397).

Venturicidin H, **2**. White powder; $[\alpha]_D^{24} + 50.00$ (c 0.40, CH₃OH); HRESIMS *m/z* 743.4695 [M + Na]⁺ (calcd for C₄₁H₆₈O₁₀Na, 743.4710).

Venturicidin I, **3**. White powder; $[\alpha]_D^{24} + 48.78$ (c 0.41, CH₃OH); HRESIMS *m/z* 753.4900 [M + NH₄]⁺ (calcd for C₄₀H₆₉N₂O₁₁, 753.4943).

Venturicidin J, **4**. White powder; $[\alpha]_D^{24} + 50.00$ (c 0.40, CH₃OH); HRESIMS *m/z* 781.5243 [M + NH₄]⁺ (calcd for C₄₂H₇₃N₂O₁₁, 781.5256).

Venturicidin G–J (**1–4**), ¹H and ¹³C NMR data (*d*₆-DMSO), see Tables 1 and 2.

Table 1. ¹H (600 MHz) NMR Data of Compounds **1–4** in *d*₆-DMSO ^a.

Position	δ_H , Mult (J in Hz)			
	1	2	3	4
2 α	2.74, d (15.6)	2.57, q (7.8)	2.76, d (16.2)	2.57, q (7.8)
2 β	2.51, overlap		2.56, d (16.2)	
2-CH ₃		1.12, overlap		1.13, d (7.2)
3-OH	5.49, s	4.93, s	5.50, overlap	4.93, s
4 α	2.16, d (17.4)	2.08, m	2.18, m	2.07, m
4 β	1.92, m	2.00, m	1.97, m	2.03, m
5	5.45, m	5.46, m	5.45, m	5.46, m
6-CH ₃	1.41, s	1.41, s	1.41, s	1.41, s
7	4.33, brs	4.30, brs	4.35, brs	4.30, brs
8-CH ₃	1.37, s	1.36, s	1.37, s	1.36, s
9	5.38, m	5.24, t (7.2)	5.50, overlap	5.41, dd (10.2, 4.2)
10 α	2.01, m	2.08, m	2.11, m	2.07, m
10 β	1.92, m	1.79, m	1.79, m	1.79, m
11 α	1.56, m	1.27, m	1.31, m	1.46, m
11 β	1.23, m	1.12, overlap	1.23, m	1.22, m
12 α	1.47, m	1.56, m	1.53, m	1.56, m
12 β	1.23, m	1.27, m	1.44, m	1.32, m
13	3.78, m	3.89, dd (12.6, 7.2)	4.02, m	3.92, m
14	5.30, dd (15.6, 8.4)	5.40, dd (10.2, 4.2)	5.28, m	5.25, m
15	5.15, dd (15.6, 9.0)	5.24, t (7.2)	5.40, m	5.25, m
16 α	1.92, m	2.00, m	2.04, m	2.07, m
16 β			1.97, m	
16-CH ₃	0.93, d (6.6)	0.90, overlap		0.91, d (6.6)
17 α	1.29, m	1.27, m	1.31, m	1.22, m
17 β	0.90, overlap	0.90, overlap	0.89, overlap	0.89, overlap
18 α	1.47, m	1.69, m	1.74, m	1.70, m
18 β	1.29, m			
18-CH ₃		0.77, d (6.6)	0.82, d (7.2)	0.77, d (6.6)
19	4.72, m	4.54, dd (6.6, 4.8)	4.64, m	4.54, m
20	1.71, m	1.79, m	1.69, m	1.79, m
20-CH ₃	0.80, d (6.6)	0.79, d (6.6)	0.81, d (7.2)	0.79, d (6.6)
21 α	1.29, m	1.27, m	1.23, m	1.32, m
21 β	0.98, m	0.95, m	0.84, d (7.2)	0.95, m
22	1.56, m	1.56, m	1.53, m	1.56, m
22-CH ₃	0.71, d (6.6)	0.72, d (6.6)	0.69, d (6.6)	0.72, d (6.6)
23	3.42, m	3.40, m	3.41, m	3.40, m
23-OH	4.88, brs		5.05, brs	5.04, brs
24	2.62, m	2.62, m	2.61, m	2.62, m
24-CH ₃	0.85, d (6.6)	0.85, d (7.2)	0.84, d (7.2)	0.85, d (7.2)
26 α	2.51, overlap	2.53, m	2.49, m	2.53, m

Table 1. Cont.

Position	δ_H , Mult (J in Hz)			
	1	2	3	4
26 β	2.01, m	2.00, m	1.97, m	2.03, m
27	0.90, overlap	0.90, overlap	0.89, overlap	0.89, overlap
1'	4.41, dd (9.6, 1.8)	4.47, dd (9.6, 1.8)	4.58, m	4.54, m
2' α	1.92, m	1.89, m	2.04, m	2.03, m
2' β	1.29, m	1.27, m	1.31, m	1.22, m
3'	4.47, m	3.40, m	4.49, m	4.47, m
3'-OH	4.88, brs			
3'-CONH ₂			6.44, brs	6.48, brs
4'	2.68, m	2.68, m	2.91, m	2.91, m
4'-OH				4.56, brs
5'	3.01, m	3.03, m	3.19, m	3.14, m
5'-CH ₃	1.10, d (6.0)	1.12, overlap	1.15, d (6.0)	1.15, d (6.0)

^a Assignments were based on COSY, HSQC and gHMBC experiments. NMR: nuclear magnetic resonance); DMSO: dimethyl sulfoxide; COSY: correlation spectroscopy; HSQC: heteronuclear singular quantum correlation); gHMBC: gradient heteronuclear multiple bond correlation.

Table 2. ¹³C (150 MHz) NMR Data of Compounds 1–4 in *d*₆-DMSO.

Position	δ_C , Type			
	1	2	3	4
1	171.7, s	176.0, s	171.9, s	176.0, s
2	44.0, t	47.6, d	43.6, t	47.6, d
2-CH ₃		13.0, q		13.0, q
3	93.5, s	95.7, s	93.4, s	95.7, s
4	34.4, t	32.7, t	34.6, t	32.7, t
5	117.5, d	117.5, d	117.5, d	117.4, d
6	131.7, s	131.9, s	131.8, s	131.9, s
6-CH ₃	18.8, q	18.9, q	18.9, q	18.9, q
7	79.2, d	79.0, d	79.1, d	79.0, d
8	134.3, s	133.5, s	134.0, s	133.6, s
8-CH ₃	11.1, q	10.7, q	10.8, q	10.7, q
9	129.3, d	129.7, d	129.1, d	129.0, d
10	26.7, t	27.2, t	26.7, t	27.1, t
11	25.3, t	25.7, t	24.7, t	25.7, t
12	29.0, t	33.9, t	32.9, t	33.8, t
13	81.3, d	80.0, d	78.4, d	80.2, d
14	131.8, d	129.0, d	131.1, d	129.6, d
15	135.7, d	138.3, d	137.4, d	138.5, d
16	37.2, d	36.4, d	30.4, t	36.4, d
16-CH ₃	21.1, q	21.6, q		21.6, q
17	32.8, t	40.4, t	34.3, t	40.4, t
18	29.0, t	32.7, d	33.9, d	32.7, d
18-CH ₃		16.5, q	12.6, q	16.5, q
19	78.3, d	82.2, d	80.9, d	82.2, d
20	31.9, d	31.2, d	31.5, d	31.2, d
20-CH ₃	16.0, q	16.2, q	15.5, q	16.2, q
21	34.6, t	35.0, t	36.8, t	35.0, t
22	31.2, d	31.3, d	31.3, d	31.3, d
22-CH ₃	11.1, q	11.0, q	10.9, q	10.9, q
23	76.0, d	76.3, d	76.3, d	76.3, d
24	49.0, d	49.1, d	48.9, d	49.1, d
24-CH ₃	13.4, q	13.4, q	13.4, q	13.4, q
25	214.4, s	214.4, s	214.5, s	214.4, s
26	35.2, t	35.2, t	35.3, t	35.2, t
27	7.4, q	7.4, q	7.4, q	7.4, q
1'	98.7, d	97.5, d	96.7, d	97.0, d
2'	40.0, t	40.0, t	37.5, t	37.5, t
3'	70.5, d	70.5, d	72.6, d	72.7, d
3'-CONH ₂			156.4, s	156.4, s
4'	76.9, d	76.9, d	73.5, d	73.5, d
5'	71.5, d	71.5, d	71.7, d	71.7, d
5'-CH ₃	18.1, q	18.1, q	18.0, q	18.0, q

2.5. Effect of Compounds on the Mycelial Growth of *P. oryzae*

Mycelial growth inhibition assay was performed as described by Li et al. [35] to measure the inhibitory effect of compounds 1–6 on *P. oryzae*. The tested compounds were dissolved in sterile water containing 0.5% DMSO and 0.25% Tween-80 to produce a desired agent concentration of 0.078125–8 µg/mL. The agents were blended with 40–45 °C potato dextrose agar, in which 0 µg/mL represented the negative control. The carbendazim was considered as the positive control. The 5 mm plugs of *P. oryzae* were placed in the center of treated plates (d = 90 mm). After 15 days of dark culture at 25 °C, the colony diameter of each test group was measured. Experiments were repeated in three replicates. The antifungal activities were calculated using the following formula:

$$\text{inhibition (\%)} = (D_C - D_T)/(D_C - 5) \times 100$$

among which, D_C is colony diameter in the negative control plate and D_T is colony diameter in the plate containing tested compounds.

2.6. Effect of Compounds on the Conidia Germination of *P. oryzae*

P. oryzae was incubated on oatmeal tomato agar medium as described by Miao et al. [36]. When *P. oryzae* reached the edge of the plate, the aerial growth was scraped off with sterilized cotton swabs. They were then placed in an incubator with black light lamp at 25 °C. After 7 days, the conidia were harvested from conidial colonies. The concentrations of conidia in suspension were adjusted to 1×10^5 conidia per mL by a hemocytometer [37] and 30 µL of various concentrations (0.078125–100 µg/mL) of tested compounds were dropped onto the glass slides with 30 µL conidial suspension before incubating both of them for 6 h. The sterile water containing 0.5% DMSO and 0.25% Tween-80 was considered as the negative control. The carbendazim was considered as the positive control. The conidia were considered to have germinated when the length of the germ tube was greater than the short radius of the conidia. When the negative control conidial germination rate was greater than 80%, the number of conidia germinated at various concentration was observed and assessed by under the microscope. Experiments were repeated in three replicates.

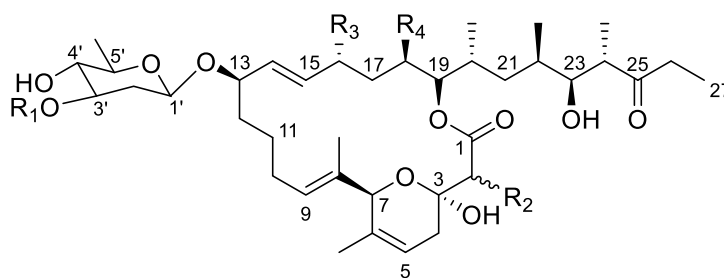
3. Results

3.1. Identification of Strain SN5452

The 16S rRNA gene sequence analysis and comparisons showed that strain SN5452 was affiliated with the genus *Streptomyces* and shared the greatest gene sequence similarity to *Streptomyces setonii* (99.79%). The phylogenetic analysis of the 16S rRNA gene sequences indicated the strain forms a cluster with *Streptomyces clavifer* NRRL B-2557^T, *Streptomyces mutomycini* NRRL B-65393^T, *Streptomyces atroolivaceus* NRRL ISP-5137^T and *Streptomyces finlayi* NRRL B-12114^T (Figure S2). Therefore, the strain SN5452 belongs to the genus *Streptomyces* and was named *Streptomyces* sp. SN5452 (Genbank accession no. ON358333).

3.2. Extraction, Separation and Purification of Extract

The CH₂Cl₂ extract from the fermentation culture of *Streptomyces* sp. SN5452 was chromatographed on silica gel column followed by further purification on Sephadex LH-20 columns and reversed-phase HPLC, to afford compounds 1–6. Analysis of ESI-MS data and ¹H and ¹³C NMR spectra suggested 5 and 6 to be venturicidins A and B, respectively, whose identities were unambiguously confirmed by extensive 2D NMR (COSY, HSQC and gHMBC) spectroscopic analyses as well as comparison to previously reported spectroscopic data (Figure 1) [38].



- 1: $R_1=R_2=R_4=H$, $R_3=CH_3$ 2: $R_1=H$, $R_2=R_3=R_4=CH_3$
- 3: $R_1=CONH_2$, $R_2=R_3=H$, $R_4=CH_3$ 4: $R_1=CONH_2$, $R_2=R_3=R_4=CH_3$
- 5: $R_1=CONH_2$, $R_2=H$, $R_3=R_4=CH_3$ 6: $R_1=R_2=H$, $R_3=R_4=CH_3$

Figure 1. Structures of compounds 1–6.

3.3. Structure Elucidation of Compounds

Compound **1** was obtained as a white powder. Its molecular formula, $C_{39}H_{64}O_{10}$, was established on the basis of HRESIMS data, indicating eight degrees of unsaturation (Figure S8). The 1H NMR spectrum of **1** showed eight methyl proton signals at δ_H 0.71–1.41 and four olefinic proton signals [δ_H 5.15 (1H, dd), 5.30 (1H, dd), 5.38 (1H, m), 5.45 (1H, m)] (Table 1 and Figure S3). The ^{13}C NMR and HSQC spectra of **1** showed eight methyl groups, ten methylene groups, sixteen methine groups, and five quaternary carbons (Figures S4 and S5). The spectroscopic data also revealed two olefinic, one ketone, one ketal and one lactone carbon signals. These results indicated that **1** possesses the same venturicinid scaffold as that of **6** (Figure 2). Analyses of the 1H and ^{13}C NMR spectra of **1** and **6** showed that one methyl group (δ_H 0.78; δ_C 12.9) and one methine group (δ_H 1.80; δ_C 34.6) found in **6** were not present in **1** (Table S1). Instead, **1** contains an additional methylene group (δ_H 1.29, 1.47; δ_C 29.0). The HMBC cross peaks of H₂-18 (δ_H 1.29, 1.47) with C-17 (δ_C 32.8) and C-19 (δ_C 78.3) indicated the methylene is located at C-18 (Figures 2 and S6). Therefore, the structure of **1** differs from that of **6** in only one aspect: the methyl group at C-18 in **6** is replaced by a proton in **1**. This was also confirmed by the HRESIMS data and molecular formulas of **1** and **6** which indicated **6** has one more carbon and two more hydrogens than **1**. The structure of compound **1** was thus elucidated, and compound **1** was named as venturicinid G.

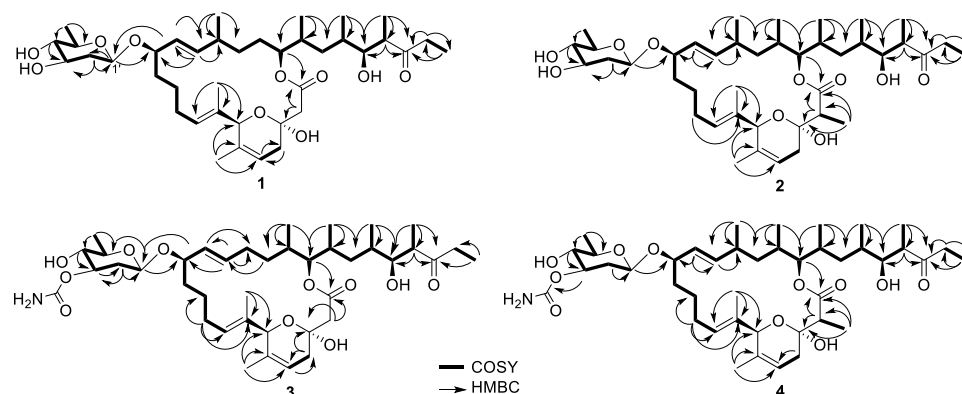


Figure 2. 2D NMR correlations of compounds 1–4. 2D NMR: two-dimensional nuclear magnetic resonance.

Compound **2** was purified as a white powder. The molecular formula of **2** was determined as $C_{41}H_{68}O_{10}$ based on HRESIMS data (Figure S15). Similarly, **2** was identified to have the same scaffold as **6** based on their spectroscopic data (Figures S9–S14). However, the 1H and ^{13}C NMR data revealed that the signals of methylene (δ_H 2.73, 2.54; δ_C 43.7)

in **6** were substituted by signals of a methyl group (δ_{H} 1.12; δ_{C} 13.0) and a methine group (δ_{H} 2.57; δ_{C} 47.6) in **2**, respectively (Table 1, Table 2 and Table S1). The HMBC correlations of $\text{H}_3\text{-2CH}_3$ (δ_{H} 1.12) with C-1 (δ_{C} 176.0), C-2 (δ_{C} 47.6) and C-3 (δ_{C} 95.7) and COSY correlation between $\text{H}_3\text{-2CH}_3$ (δ_{H} 1.12) and H-2 (δ_{H} 2.57) illustrated the position of the methyl at C-2 (Figure 2). From these results, the structure of compound **2** was elucidated, and compound **2** was named as venturicidin H.

Compound **3** was obtained as white powder. Its molecular formula, $\text{C}_{40}\text{H}_{65}\text{NO}_{11}$, was inferred by HRESIMS data (Figure S21). The NMR data exhibited structure of **3** was highly similar to that of **5** (Figure S16–S20). The analysis of ^1H NMR data of **5** exhibited a methyl ($\text{H}_3\text{-16CH}_3$, δ_{H} 0.89) that was absent in **3**, while **3** had a methylene at $\text{H}_2\text{-16}$ (δ_{H} 2.04, 1.97) rather than a methine at H-16 (δ_{H} 2.06) in **5** (Tables 1 and S1). The HMBC correlations of $\text{H}_2\text{-16}$ with C-15 (δ_{C} 137.4) and C-17 (δ_{C} 34.3) also revealed the methyl (δ_{H} 0.89) in **5** was missing in **3** (Figure 2), corresponding to a 14 Da mass decrease. Consequently, **3** was elucidated and named as venturicidin I.

Compound **4** was isolated as white powder, and revealed spectroscopic data remarkable similar with those of **5** (Figure S22–S27). The molecular formula of **4** was determined as $\text{C}_{42}\text{H}_{69}\text{NO}_{11}$ compatibly with its HRESIMS data (Figure S28), which was 14 amu higher than that of **5**, suggesting the presence of an additional methyl group (δ_{H} 1.13, δ_{C} 13.0) in **4** (Tables 1 and 2). The HMBC correlations of $\text{H}_3\text{-2CH}_3$ (δ_{H} 1.13) with C-1 (δ_{C} 176.0), C-2 (δ_{C} 47.6) and C-3 (δ_{C} 95.7) and COSY correlation between $\text{H}_3\text{-2CH}_3$ (δ_{H} 1.13) and H-2 (δ_{H} 2.57) confirmed that the additional methyl was located at C-2 of **4** (Figure 2). Therefore, the structure of **4** was determined as illustrated in Figure 1, and compound **4** was named as venturicidin J.

3.4. Antifungal Activity Assay

Compounds **1–6** were evaluated for their antifungal activities against *P. oryzae* in mycelial growth inhibition and conidial germination assays. The results showed EC_{50} values of the compounds **1–6** against mycelial growth were approximately 1.78, 1.43, 0.35, 1.40, 0.11, 0.15 $\mu\text{g}/\text{mL}$, respectively (Table 3). Notably, the compounds **3**, **5** and **6** remarkably limit the mycelial radial elongation of *P. oryzae* (Figure 3), which showed comparable antifungal activity to the positive control carbendazim ($\text{EC}_{50} = 0.30 \mu\text{g}/\text{mL}$). Compounds **1**, **2** and **4** showed moderate antifungal activities.

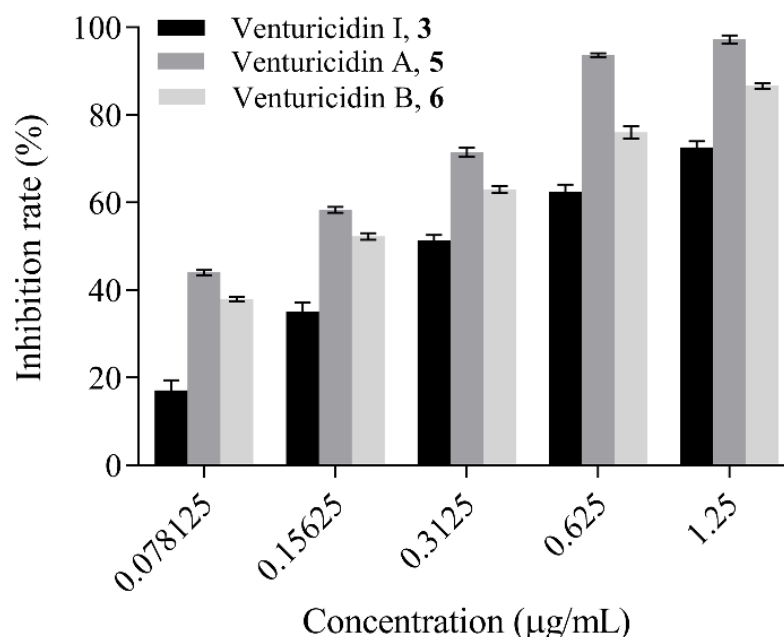


Figure 3. Effect of venturicidin I, **3**, venturicidin A, **5**, and venturicidin B, **6** on mycelial growth of *P. oryzae*.

Table 3. Half maximal effective concentration (EC₅₀) values of Compounds 1–6 on *P. oryzae*^a.

Compound	Mycelial Growth Inhibition EC ₅₀ , µg/mL (±SD)	Conidial Germination Inhibition EC ₅₀ , µg/mL (±SD)
venturicidin G, 1	1.78 ± 0.09	24.95 ± 1.63
venturicidin H, 2	1.43 ± 0.02	5.55 ± 0.12
venturicidin I, 3	0.35 ± 0.03	1.14 ± 0.03
venturicidin J, 4	1.40 ± 0.09	4.49 ± 0.28
venturicidin A, 5	0.11 ± 0.00	0.27 ± 0.02
venturicidin B, 6	0.15 ± 0.01	0.39 ± 0.01
Carbendazim ^b	0.30 ± 0.01	3.99 ± 0.08

^a Data shown are the mean of three independent experiments and presented as mean ± standard deviation (SD).

^b Positive control.

In addition to inhibiting mycelial growth, compounds 1–6 also inhibited the conidial germination of *P. oryzae* in different levels, with the EC₅₀ values estimated to be 24.95, 5.55, 1.14, 4.49, 0.27 and 0.39 µg/mL, respectively (Table 3). These results indicated that compounds 5 and 6 exert higher antimicrobial activity against *P. oryzae* than the positive control carbendazim (EC₅₀ = 3.99 µg/mL). Compounds 2, 3 and 4 showed comparable antifungal activity to the positive control, and compound 1 exhibited weaker inhibitory activity than carbendazim.

3.5. Structure Activity Relationship Analysis

The relationship between the structures and antifungal activity was elucidated based on the compounds' molecular structures, and the discussion upon their antimicrobial activity results against different developmental stages of *P. oryzae*. Both compounds 5 and 6 showed similar antifungal activity against *P. oryzae*, indicating the presence of acylamino group at the C-3 position does not cause a prominent effect on its activity. Comparing the structures of 1 with 6, a methyl group at the C-18 (R₄) was replaced by a hydrogen atom in 1, which impairs the antifungal activity against *P. oryzae*, so they have large activity differences in conidial germination inhibition. In contrast, between 3 and 5 the replacement in 3 happened on C-16 (R₃), which indicates that they have no differences in antifungal activity. Thus, the methyl group in position R₄ seems to increase the activity. Both compounds 2 and 4 introduce a methyl group at the C-2 position, lower the antimicrobial activity in comparison with that of 5 and 6. These results suggested that the antifungal activities of these compounds are influenced by the methylated positions in venturicidins. The SARs of these compounds provided a scientific basis for discovery of potent fungicides.

4. Discussion

With the increasing devastating rice blast disease, *P. oryzae* has provoked severe loss in the world [39]. The control of rice blast remains a long-standing agricultural issue associated with highly variable nature of *P. oryzae* [37,40]. In addition, *P. oryzae* has developed resistance to most of commercially available fungicides [16]. Thus, novel fungicides are a constant and critical need. Recently, microbial pesticides are widely applied in the control of plant diseases due to friendliness to the environment [41]. Unfortunately, there are few reports on the microbial pesticides against *P. oryzae*. This study indicated that secondary metabolites of *Streptomyces* sp. SN5452 may be promising fungicides in the control of rice blast, because they strongly inhibit the mycelial growth and the conidial germination of *P. oryzae*. The isolation and screening of *Streptomyces* are the prerequisites for obtaining bioactive natural products [42]. In our study, *Streptomyces* sp. SN5452 was isolated and purified from the gut of a millipede. By the analysis of 16S rRNA gene sequence, the strain belonged to *Streptomyces* genus, and the crude extract made from the fermentation culture of the strain showed prominent inhibitory activity against *P. oryzae*.

Streptomyces produce a number of secondary metabolites used in fields. The commercial kasugamycin produced by *Streptomyces kasugaensis* showed potential preventive effects against rice blast [43]. The insecticide avermectin has been used extensively for

controlling *Plutella xylostella* and *Pieris rapae* in fields, which was produced by *Streptomyces avermitilis* [44–46]. Furthermore, *Streptomyces* fermentation products are considered as a valuable resource for the development of novel pesticides. The dimethyl sulfide and trimethyl sulfide produced by *Streptomyces* sp. AN090126, showed broad-spectrum antimicrobial activity against various plant-pathogenic bacteria and fungi, including *Ralstonia solanacearum*, *Xanthomonas euvesicatoria*, *Sclerotinia homoeocarpa* [47]. The LC₅₀ value of endostemonine J, an ionophore antibiotic produced by *Streptomyces* sp. BS-1, against *Aphis gossypii* was 3.55 µg/mL at 72 h via leaf dipping assay [48]. Compound cinnoline-4-carboxylic acid was isolated from the fermentation culture of *Streptomyces* sp. KRA17-580 by Kim's group, and completely inhibited the growth *Digitaria ciliaris* at a concentration of 50 µg/mL [49]. In this study, venturicidins A, B and venturicidins G–J were isolated from the fermentation culture of *Streptomyces* sp. SN5452. These compounds inhibited mycelial growth and conidial germination of *P. oryzae*, with EC₅₀ values ranging from 0.11 to 1.78 µg/mL and from 0.27 to 24.95 µg/mL, respectively.

As we all know, structures of compounds were determined by the cumulative analyses of NMR, MS and X-ray data. The current study showed that the absolute configuration of compounds 1, 3, 5 and 6 were elucidated based on NMR and MS analyses and previously reported X-ray data [46]. However, the absolute configuration of compounds 2 and 4 were uncertain by spectroscopic data. We also tried to cultivate single-crystals of the compounds 2 and 4, but unfortunately it was not successful due to their structural specificity. Named as venturicidins G–J, compounds 1–4 enriched the structural diversity of 20-membered macrolide compounds [50–55], and compounds 5–6 were identified as venturicidins A–B. Further, venturicidins A, B and I exhibited good inhibition to mycelial growth and conidial germination of *P. oryzae*, which was comparable or superior to the positive control carbendazim. However, the actual field efficacy of these compounds should be further studied.

5. Conclusions

In conclusion, the crude extract made from the fermentation culture of *Streptomyces* sp. SN5452 showed inhibitory activity against *P. oryzae*. Compounds 1, 2, 3 and 4 were isolated and identified for the first time from the fermentation culture of *Streptomyces* sp. SN5452. Compounds 3, 5 and 6 exhibited good antimicrobial activity against *P. oryzae*. Given that microbial secondary metabolites exhibit excellent fungicide activity, they have the potential to become lead molecules for agricultural fungicides.

Supplementary Materials: The following supporting information can be downloaded at: <https://www.mdpi.com/article/10.3390/microorganisms10081612/s1>, Table S1: ¹H (600 MHz) and ¹³C (150 MHz) NMR Data of Compounds 5 and 6 in *d*₆-DMSO; Figure S1: Effects of crude extract of *Streptomyces* sp. SN5452 on the mycelial growth of *P. oryzae*; Figure S2: Neighbour-joining phylogenetic tree based on the 16S rRNA gene sequences with members of the genus *Streptomyces*; Figures S3–S28: HRESI-MS and NMR spectra of compounds 1–4.

Author Contributions: Conceptualization, Y.W. and D.Y.; methodology, Y.W.; software, Y.W. and Y.B.; validation, D.Y. and Y.B.; formal analysis, Y.W. and D.Y.; investigation, Y.B.; resources, D.Y.; writing—original draft preparation, Y.W.; writing—review and editing, Z.Y.; supervision, Y.B. and Z.Y. All authors have read and agreed to the published version of the manuscript.

Funding: This research was funded by the Innovation & Cultivation Project for Postgraduate of Shenyang Agricultural University in 2021 (grant number 2021YCXB17).

Institutional Review Board Statement: Not applicable.

Informed Consent Statement: Not applicable.

Data Availability Statement: Not applicable.

Acknowledgments: The authors thank Yongming Yan of Shenzhen University for technical assistance with NMR and MS spectra.

Conflicts of Interest: The authors declare no conflict of interest.

References

1. Godfray, H.C.J.; Beddington, J.R.; Crute, I.R.; Haddad, L.; Lawrence, D.; Muir, J.F.; Pretty, J.; Robinson, S.; Thomas, S.M.; Toulmin, C. Food security: The challenge of feeding 9 billion people. *Science* **2010**, *327*, 812–818. [[CrossRef](#)] [[PubMed](#)]
2. Muthayya, S.; Sugimoto, J.D.; Montgomery, S.; Maberly, G.F. An overview of global rice production, supply, trade, and consumption. *Ann. N. Y. Acad. Sci.* **2014**, *1324*, 7–14. [[CrossRef](#)] [[PubMed](#)]
3. Sakulkoo, W.; Osés-Ruiz, M.; Garcia, O.E.; Soanes, D.M.; Littlejohn, G.R.; Hacker, C.; Correia, A.; Valent, B.; Talbot, N.J. A single fungal MAP kinase controls plant cell-to-cell invasion by the rice blast fungus. *Science* **2018**, *359*, 1399–1403. [[CrossRef](#)] [[PubMed](#)]
4. Talbot, N.J. On the trail of a cereal killer: Exploring the biology of *Magnaporthe grisea*. *Annu. Rev. Microbiol.* **2003**, *57*, 177–202. [[CrossRef](#)]
5. Lam, V.B.; Meyer, T.; Arias, A.A.; Ongena, M.; Oni, F.E.; Höfte, M. *Bacillus* cyclic lipopeptides Iturin and Fengycin control rice blast caused by *Pyricularia oryzae* in potting and acid sulfate soils by direct antagonism and induced systemic resistance. *Microorganisms* **2021**, *9*, 1441. [[CrossRef](#)]
6. Odjo, T.; Diagne, D.; Adreit, H.; Milazzo, J.; Raveloson, H.; Andriantsimalona, D.; Kassankogno, A.I.; Ravel, S.; Gumedzoé, Y.M.D.; Ouedraogo, I.; et al. Structure of African populations of *Pyricularia oryzae* from rice. *Phytopathology* **2021**, *111*, 1428–1437. [[CrossRef](#)]
7. Dang, Y.J.; Wei, Y.; Wang, Y.Y.; Liu, S.S.; Julia, C.; Zhang, S.H. Cleavage of PrePL by Lon promotes growth and pathogenesis in *Magnaporthe oryzae*. *Environ. Microbiol.* **2021**, *23*, 4881–4895. [[CrossRef](#)]
8. Manandhar, H.K.; Jorgensen, H.J.L.; Smedegaard-Petersen, V.; Mathur, S.B. Seedborne infection of rice by *Pyricularia oryzae* and its transmission to seedlings. *Plant Dis.* **1998**, *82*, 1093–1099. [[CrossRef](#)]
9. Hayashi, K.; Yoshida, T.; Hayano-Saito, Y. Detection of white head symptoms of panicle blast caused by *Pyricularia oryzae* using cut-flower dye. *Plant Methods* **2019**, *15*, 159. [[CrossRef](#)]
10. Langner, T.; Bialas, A.; Kamoun, S. The blast fungus decoded: Genomes in flux. *mBio* **2018**, *9*, e00571–18. [[CrossRef](#)]
11. Law, J.W.; Ser, H.L.; Khan, T.M.; Chuah, L.H.; Pusparajah, P.; Chan, K.G.; Goh, B.H.; Lee, L.H. The potential of *Streptomyces* as biocontrol agents against the rice blast fungus, *Magnaporthe oryzae* (*Pyricularia oryzae*). *Front. Microbiol.* **2017**, *8*, 3. [[CrossRef](#)]
12. Kunova, A.; Pizzatti, C.; Cortesi, P. Impact of tricyclazole and azoxystrobin on growth, sporulation and secondary infection of the rice blast fungus, *Magnaporthe oryzae*. *Pest Manag. Sci.* **2013**, *69*, 278–284. [[CrossRef](#)]
13. Asibi, A.E.; Chai, Q.; Coulter, J.A. Rice blast: A disease with implications for global food security. *Agronomy* **2019**, *9*, 451. [[CrossRef](#)]
14. Peng, Q.; Zhao, H.; Zhao, G.; Gao, X.; Miao, J.; Liu, X. Resistance assessment of pyraoxystrobin in *Magnaporthe oryzae* and the detection of a point mutation in *cyt b* that confers resistance. *Pestic. Biochem. Physiol.* **2022**, *180*, 105006. [[CrossRef](#)]
15. Li, C.; Wang, K.; Zhang, H.; Yang, D.; Deng, Y.; Wang, Y.; Qi, Z. Development of a LAMP method for detecting F129L mutant in azoxystrobin-resistant *Pyricularia oryzae*. *Fungal Biol.* **2022**, *126*, 47–53. [[CrossRef](#)]
16. Zheng, F.; Li, Y.C.; Zhang, Z.X.; Jia, J.L.; Hu, P.T.; Zhang, C.Q.; Xu, H.H. Novel strategy with an eco-friendly polyurethane system to improve rainfastness of tea saponin for highly efficient rice blast control. *J. Clean. Prod.* **2020**, *264*, 121685. [[CrossRef](#)]
17. Pooja, K.; Katoch, A. Past, present and future of rice blast management. *Plant Sci. Today* **2014**, *1*, 165–173. [[CrossRef](#)]
18. Yoon, M.Y.; Cha, B.; Kim, J.C. Recent trends in studies on botanical fungicides in agriculture. *Plant Pathol. J.* **2013**, *29*, 1–9. [[CrossRef](#)]
19. Palaniyandi, S.A.; Yang, S.H.; Zhang, L.X.; Suh, J.W. Effects of actinobacteria on plant disease suppression and growth promotion. *Appl. Microbiol. Biotechnol.* **2013**, *97*, 9621–9636. [[CrossRef](#)]
20. Chaiharn, M.; Theantana, T.; Pathom-Aree, W. Evaluation of biocontrol activities of *Streptomyces* spp. against rice blast disease fungi. *Pathogens* **2020**, *9*, 126. [[CrossRef](#)]
21. Zhao, J.W.; Han, L.Y.; Yu, M.Y.; Cao, P.; Li, D.M.; Guo, X.W.; Liu, Y.Q.; Wang, X.J.; Xiang, W.J. Characterization of *Streptomyces sporangiiformans* sp. nov., a novel soil actinomycete with antibacterial activity against *Ralstonia solanacearum*. *Microorganisms* **2019**, *7*, 360. [[CrossRef](#)]
22. Yadav, A.N.; Verma, P.; Kumar, S.; Kumar, V.; Kumar, M.; Chellammal, T.; Sugitha, K.; Singh, B.P.; Saxena, A.K.; Dhaliwal, H.S. Actinobacteria from Rhizosphere: Molecular Diversity, Distributions, and Potential Biotechnological Applications. In *New and Future Developments in Microbial Biotechnology and Bioengineering*; Elsevier: Amsterdam, The Netherlands, 2018; pp. 13–41.
23. Hwang, K.S.; Kim, H.U.; Charusanti, P.; Palsson, B.Ø.; Lee, S.Y. Systems biology and biotechnology of *Streptomyces* species for the production of secondary metabolites. *Biotechnol. Adv.* **2014**, *32*, 255–268. [[CrossRef](#)]
24. Copping, L.G.; Duke, S.O. Natural products that have been used commercially as crop protection agents. *Pest Manag. Sci.* **2007**, *63*, 524–554. [[CrossRef](#)]
25. Han, C.Y.; Yu, Z.Y.; Zhang, Y.T.; Wang, Z.Y.; Zhao, J.W.; Huang, S.X.; Ma, Z.H.; Wen, Z.Y.; Liu, C.X.; Xiang, W.S. Discovery of Frenolicin B as potential agrochemical fungicide for controlling *Fusarium* head blight on wheat. *J. Agric. Food Chem.* **2021**, *69*, 2108–2117. [[CrossRef](#)]
26. Shi, L.Q.; Wu, Z.Y.; Zhang, Y.N.; Zhang, Z.G.; Fang, W.; Wang, Y.Y.; Wan, Z.Y.; Wang, K.M.; Ke, S.Y. Herbicidal secondary metabolites from actinomycetes: Structure diversity, modes of action, and their roles in the development of herbicides. *J. Agric. Food Chem.* **2020**, *68*, 17–32. [[CrossRef](#)]
27. Kaur, T.; Vasudev, A.; Sohal, S.K.; Manhas, R.K. Insecticidal and growth inhibitory potential of *Streptomyces hydrogenans* DH16 on major pest of India, *Spodoptera litura* (Fab.) (Lepidoptera: Noctuidae). *BMC Microbiol.* **2014**, *14*, 227. [[CrossRef](#)]

28. Bi, Y.H.; Yu, Z.G. Diterpenoids from *Streptomyces* sp. SN194 and their antifungal activity against *Botrytis cinerea*. *J. Agric. Food Chem.* **2016**, *64*, 8525–8529. [[CrossRef](#)]
29. Tian, H.; Shafi, J.; Ji, M.S.; Bi, Y.H.; Yu, Z.G. Antimicrobial metabolites from *Streptomyces* sp. SN0280. *J. Nat. Prod.* **2017**, *80*, 1015–1019. [[CrossRef](#)]
30. Heo, J.; Hamada, M.; Cho, H.; Weon, H.Y.; Kim, J.S.; Hong, S.B.; Kim, S.J.; Kwon, S.W. *Weissella cryptocerci* sp. nov., isolated from gut of the insect *Cryptocercus kyebangensis*. *Int. J. Syst. Evol. Microbiol.* **2019**, *69*, 2801–2806. [[CrossRef](#)]
31. Saitou, N.; Nei, M. The neighbor-joining method: A new method for reconstructing phylogenetic trees. *Mol. Biol. Evol.* **1987**, *4*, 406–425.
32. Kumar, S.; Stecher, G.; Tamura, K. Mega7: Molecular evolutionary genetics analysis version 7.0 for bigger datasets. *Mol. Biol. Evol.* **2016**, *33*, 1870–1874. [[CrossRef](#)] [[PubMed](#)]
33. Atlas, R.M. *The Handbook of Microbiological Media for the Examination of Food*, 2nd ed.; CRC Press: Boca Raton, FL, USA, 2006. [[CrossRef](#)]
34. Shirling, E.B.; Gottlieb, D. Methods for characterization of *Streptomyces* species. *Int. J. Syst. Bacteriol.* **1966**, *16*, 313–340. [[CrossRef](#)]
35. Li, R.Y.; Wu, X.M.; Yin, X.H.; Long, Y.H.; Li, M. Naturally produced citral can significantly inhibit normal physiology and induce cytotoxicity on *Magnaporthe grisea*. *Pestic. Biochem. Physiol.* **2015**, *118*, 19–25. [[CrossRef](#)] [[PubMed](#)]
36. Miao, J.Q.; Zhao, G.S.; Wang, B.; Du, Y.X.; Li, Z.W.; Gao, X.H.; Zhang, C.; Liu, X.L. Three point-mutations in cytochrome *b* confer resistance to trifloxystrobin in *Magnaporthe oryzae*. *Pest Manag. Sci.* **2020**, *76*, 4258–4267. [[CrossRef](#)]
37. Macieli, J.L.; Ceresini, P.C.; Castroagudin, V.L.; Zala, M.; Kema, G.H.; McDonald, B.A. Population structure and pathotype diversity of the wheat blast pathogen *Magnaporthe oryzae* 25 years after its emergence in Brazil. *Phytopathology* **2014**, *104*, 95–110. [[CrossRef](#)]
38. Shaaban, K.A.; Singh, S.; Elshahawi, S.I.; Wang, X.C.; Ponomareva, L.V.; Sunkara, M.; Copley, G.C.; Hower, J.C.; Morris, A.J.; Kharel, M.K.; et al. Venturicin C, a new 20-membered macrolide produced by *Streptomyces* sp. TS-2-2. *J. Antibiot.* **2014**, *67*, 223–230. [[CrossRef](#)]
39. Chadha, S. Molecular detection of *Magnaporthe oryzae* from rice seeds. *Methods Mol. Biol.* **2021**, *2356*, 187–197.
40. Park, S.Y.; Milgroom, M.G.; Han, S.S.; Kang, S.; Lee, Y.H. Genetic differentiation of *Magnaporthe oryzae* populations from scouting plots and commercial rice fields in Korea. *Phytopathology* **2008**, *98*, 436–442. [[CrossRef](#)]
41. Ling, L.; Han, X.Y.; Li, X.; Zhang, X.; Wang, H.; Zhang, L.D.; Cao, P.; Wu, Y.T.; Wang, X.J.; Zhao, J.W.; et al. A *Streptomyces* sp. NEAU-HV9: Isolation, identification, and potential as a biocontrol agent against *Ralstonia Solanacearum* of tomato plants. *Microorganisms* **2020**, *8*, 351. [[CrossRef](#)]
42. Montesinos, E. Development, registration and commercialization of microbial pesticides for plant protection. *Int. Microbiol.* **2003**, *6*, 245–252. [[CrossRef](#)]
43. Umezawa, H.; Hamada, M.; Suhara, Y.; Hashimoto, T.; Ikekawa, T. Kasugamycin, a new antibiotic. *J. Antibiot.* **1965**, *18*, 101–104.
44. Kaziem, A.E.; Gao, Y.H.; Zhang, Y.; Qin, X.Y.; Xiao, Y.N.; Zhang, Y.H.; You, H.; Li, J.H.; He, S. α -Amylase triggered carriers based on cyclodextrin anchored hollow mesoporous silica for enhancing insecticidal activity of avermectin against *Plutella xylostella*. *J. Hazard Mater.* **2018**, *359*, 213–221. [[CrossRef](#)]
45. Wang, P.; Lu, Y.; Dong, J.; Jing, L.; Yuan, Z.Q.; Yang, J.G.; Qiao, Y. Control effect of 13 pesticides on *Pieris rapae* in the cauliflower field. *Agrochemicals* **2017**, *56*, 300–302.
46. Burg, R.W.; Miller, B.M.; Baker, E.E.; Birnbaum, J.; Currie, S.A.; Hartman, R.; Kong, Y.L.; Monaghan, R.L.; Olson, G.; Putter, I.; et al. Avermectins, new family of potent anthelmintic agents: Producing organism and fermentation. *Antimicrob. Agents Chemother.* **1979**, *15*, 361–367. [[CrossRef](#)]
47. Le, K.D.; Yu, N.H.; Park, A.R.; Park, D.J.; Kim, C.J.; Kim, J.C. *Streptomyces* sp. AN090126 as a biocontrol agent against bacterial and fungal plant diseases. *Microorganisms* **2022**, *10*, 791. [[CrossRef](#)]
48. Zhao, H.M.; Yang, A.P.; Zhang, N.; Li, S.Y.; Yuan, T.J.; Ding, N.; Zhang, S.W.; Bao, S.; Wang, C.; Zhang, Y.N.; et al. Insecticidal endostemonines A–J produced by endophytic *Streptomyces* from *Stemona sessilifolia*. *J. Agric. Food Chem.* **2020**, *68*, 1588–1595. [[CrossRef](#)]
49. Kim, H.J.; Bo, A.B.; Kim, J.D.; Kim, Y.S.; Khaitov, B.; Ko, Y.K.; Cho, K.M.; Jang, K.S.; Park, K.W.; Choi, J.S. Herbicidal characteristics and structural identification of the potential active compounds from *Streptomyces* sp. KRA17-580. *J. Agric. Food Chem.* **2020**, *68*, 15373–15380. [[CrossRef](#)]
50. Brufani, M.; Cerrini, S.; Fedeli, W.; Musu, C.; Cellai, L.; Keller-Schierlein, W. Structures of the venturicin A and B. *Experientia* **1971**, *27*, 604–606. [[CrossRef](#)]
51. Omura, S.; Tanaka, Y.; Nakagawa, A.; Iwai, Y.; Inoue, M.; Tanaka, H. Irumamycin, a new antibiotic active against phytopathogenic fungi. *J. Antibiot.* **1982**, *35*, 256–257. [[CrossRef](#)]
52. Omura, S.; Nakagawa, A.; Imamura, N.; Kushida, K.; Liu, C.M.; Sello, L.H.; Westley, J.W. Structure of a new macrolide antibiotic, X-14952B. *J. Antibiot.* **1985**, *38*, 674–676. [[CrossRef](#)]
53. Ohta, S.; Uy, M.M.; Yanai, M.; Ohta, E.; Hirata, T.; Ikegami, S. Exiguolide, a new macrolide from the marine sponge *Geodia exigua*. *Tetrahedron Lett.* **2006**, *47*, 1957–1960. [[CrossRef](#)]
54. Peng, F.; Wang, C.X.; Xie, Y.; Jing, H.L.; Che, L.J.; Uribe, P.; Bull, A.T.; Goodfellow, M.; Jiang, H.; Lian, Y.Y. A new 20-membered macrolide produced by a marine-derived *Micromonospora* strain. *Nat. Prod. Res.* **2013**, *27*, 1366–1371.
55. Li, H.H.; Zhang, M.X.; Li, H.J.; Yu, H.; Chen, S.; Wu, W.H.; Sun, P. Discovery of venturicin congeners and identification of the biosynthetic gene cluster from *Streptomyces* sp. NRRL S-4. *J. Nat. Prod.* **2021**, *84*, 110–119. [[CrossRef](#)]